

Single-cycle radio-frequency pulse generation by an optoelectronic oscillator

Etgar C. Levy,^{1,*} and Moshe Horowitz¹

¹*Department of Electrical Engineering, Technion—Israel Institute of Technology, Haifa 32000 Israel*

[*etgarlevy@gmail.com](mailto:etgarlevy@gmail.com)

Abstract: We demonstrate experimentally passive mode-locking of an optoelectronic oscillator which generates a single-cycle radio-frequency pulse train. The measured pulse to pulse jitter was less than 5 ppm of the round-trip duration. The pulse waveform was repeated each round-trip. This result indicates that the relative phase between the pulse envelope and the carrier wave is autonomously locked. The results demonstrate, for the first time, that single-cycle pulses can be directly generated by a passive mode-locked oscillator. The passive mode-locked optoelectronic oscillator is important for developing novel radars and radio-frequency pulsed sources and it enables studying directly the physics of single-cycle pulse generation.

© 2011 Optical Society of America

OCIS codes: (230.0250) Optoelectronics; (140.4050) Mode-locked lasers; (230.4910) Oscillators; (320.5550) Pulses.

References and links

1. A. J. DeMaria, D. A. Stetsen, and H. Heyman, "Experimental study of mode-locked Ruby laser," *Appl. Phys. Lett.* **8**, 22 (1966).
2. C. V. Shank and E. P. Ippen, "Subpicosecond kilowatt pulses from a mode-locked cw dye laser," *Appl. Phys. Lett.* **24**, 373–375 (1974).
3. S. Namiki, X. Yu, and H. A. Haus, "Observation of nearly quantum-limited timing jitter in an all-fiber ring laser," *J. Opt. Soc. Am. B* **13**, 2817–2823 (1996).
4. H. A. Haus, "Theory of mode locking with a fast saturable absorber," *J. Appl. Phys.* **46**, 3049–3058 (1975).
5. U. Morgner, F. X. Kärtner, S. H. Cho, Y. Chen, H. A. Haus, J. G. Fujimoto, E. P. Ippen, V. Scheuer, G. Angelow, and T. Tschudi, "Sub-two-cycle pulses from a Kerr-lens mode-locked Ti:sapphire laser," *Opt. Lett.* **24**, 411–413 (1999).
6. D. H. Sutter, G. Steinmeyer, L. Gallmann, N. Matuschek, F. Morier-Genoud, U. Keller, V. Scheuer, G. Angelow, and T. Tschudi, "Semiconductor saturable-absorber mirror-assisted Kerr-lens mode-locked Ti:sapphire laser producing pulses in the two-cycle regime," *Opt. Lett.* **24**, 631–633 (1999).
7. S. Rausch, T. Binhammer, A. Harth, F. X. Kärtner, and U. Morgner, "Controlled waveforms on the single-cycle scale from a femtosecond oscillator," *Opt. Express* **16**, 17410–17419 (2008).
8. M. Y. Shverdin, D. R. Walker, D. D. Yavuz, G. Y. Yin, and S. E. Harris, "Generation of a single-cycle optical pulse," *Phys. Rev. Lett.* **94**, 033904 (2005).
9. E. Goulielmakis, M. Schultze, M. Hofstetter, V. S. Yakovlev, J. Gagnon, M. Uiberacker, A. L. Aquila, E. M. Goulikson, D. T. Attwood, R. Kienberger, F. Krausz, and U. Kleineberg, "Single-cycle nonlinear optics," *Science* **320**, 1614–1617 (2008).
10. G. Krauss, S. Lohss, T. Hanke, A. Sell, S. Eggert, R. Huber, and A. Leitenstorfer, "Synthesis of a single cycle of light with compact erbium-doped fibre technology," *Nat. Photonics* **4**, 33–36 (2010).
11. X. S. Yao and L. Maleki, "Optoelectronic microwave oscillator," *J. Opt. Soc. Am. B* **13**, 1725–1735 (1996).
12. N. Yu, E. Salik, and L. Maleki, "Ultralow-noise mode-locked laser with coupled optoelectronic oscillator configuration," *Opt. Lett.* **15**, 1231–1233 (1995).

13. J. Lasri, A. Bilenca, D. Dahan, V. Sidorov, G. Eisenstein, D. Ritter, K. Yvind, "Self-starting hybrid optoelectronic oscillator generating ultra low jitter 10-GHz optical pulses and low phase noise electrical signals," *IEEE Photon. Technol. Lett.* **14**, 1004–1006 (2002).
14. Y. K. Chembo, A. Hmima, P. Lacourt, L. Larger, and J. M. Dudley, "Generation of ultralow jitter optical pulses using optoelectronic oscillators with time-lens soliton-assisted compression," *J. Lightwave Technol.* **27**, 5160–5167 (2009).
15. J. Lasri, P. Devgan, R. Tang, and P. Kumar, "Self-starting optoelectronic oscillator for generating ultra-low-jitter high-rate (10 GHz or higher) optical pulses," *Opt. Express* **11**, 1430–1435 (2003).
16. A. F. Kardo-Sysoev, "New power semiconductor Devices for generation of nano- and subnanosecond pulses," in *Ultra-wideband radar technology*, J. D. Taylor Ed. (CRC, 2001), ch. 9.
17. M. H. Khan, H. Shen, Y. Xuan, L. Zhao, S. Xiao, D. E. Leaird, A. M. Weiner, and M. Qi, "Ultrabroad-bandwidth arbitrary radiofrequency waveform generation with a silicon photonic chip-based spectral shaper," *Nat. Photonics* **4**, 117–122 (2010).
18. C. C. Cutler, "The regenerative pulse generator," *Proc. IRE*, **43**, 140–148 (1955).
19. D. J. Jones, S. A. Diddams, J. K. Ranka, A. Stentz, R. S. Windeler, J. L. Hall, and S. T. Cundiff, "Carrier-envelope phase control of femtosecond mode-locked lasers and direct optical frequency synthesis," *Science* **288**, 635–639 (2000).
20. J. Yao, F. Zeng, and Q. Wang, "Photonic generation of ultrawideband signals," *J. Lightwave Technol.* **25**, 3219–3235 (2007).
21. J. Li, Y. Liang, and K. Kin-Yip Wong, "Millimeter-wave UWB signal generation via frequency up-conversion using fiber optical parametric amplifier," *IEEE Photon. Technol. Lett.* **21**, 1172–1174 (2009).
22. F. Zhang, J. Wu, S. Fu, K. Xu, Y. Li, X. Hong, P. Shum, and J. Lin "Simultaneous multi-channel CMW-band and MMW-band UWB monocycle pulse generation using FWM effect in a highly nonlinear photonic crystal fiber," *Opt. Express* **17**, 15870–15875 (2010).
23. H. A. Haus, and A. Mecozzi, "Noise of mode-locked lasers," *IEEE J. Quantum Electron.* **29**, 983–996 (1993).
24. M. E. Grein, H. A. Haus, Y. Chen, and E. P. Ippen, "Quantum-limited timing jitter in actively modelocked lasers," *IEEE J. Quantum Electron.* **40**, 1458–1470 (2004).
25. V. S. Grigoryan, C. R. Menyuk, and R.-M. Mu "Calculation of timing and amplitude jitter in dispersion-managed optical fiber communications using linearization," *J. Lightwave Technol.* **17**, 1347–1356 (1999).
26. M. I. Skolnik, *Introduction to Radar Systems*, 2nd ed. (McGraw-Hill, 1981), pp. 553–560.

1. Introduction

Passive mode-locking in lasers is used to generate ultrashort pulse train [1,2] with a timing jitter that can be close to its quantum limit value [3]. Ultrashort pulses that are generated by passive mode-locking are obtained by inserting a fast saturable absorber into a laser cavity [2,4]. The transmission of such an absorber increases as the intensity of the light increases. Therefore, the absorber promotes the laser to generate short intense pulses with a broad spectrum instead of generating a continuous wave signal with a low peak power. From the frequency domain point of view, the saturable absorber locks the phases of the laser modes to obtain short pulses. The shortest pulse duration that was demonstrated in passive mode-locked lasers was limited to few cycles of the carrier wave [5–7]. To generate single-cycle optical pulses there is a need to utilize techniques that are based on coherent control of four-wave-mixing [8], nonlinear optic [9], or combining laser sources [10].

Optoelectronic oscillators (OEOs) are hybrid devices in which the signal propagates alternately in optical and in electronic components [11]. Due to the low loss in optical fibers, they are utilized as a long delay-line that increases the quality factor of the OEO. As a result, OEOs can generate continuous wave signals at frequencies up to tens of GHz with extremely low phase-noise [11]. Coupled-OEOs generate ultra-low jitter optical pulses, which propagate through an all-optical path that contains an electro-optic modulator that is fed by an electrical continuous wave [12]. Short optical pulses can also be obtained by soliton-assisted compression of sinusoidally modulated prepulses generated by an OEO [13, 14] or by using an electro-absorption modulator [15]. In all of those works a narrowband electrical filter is used to eliminate most of the cavity modes.

Generating low-jitter single-cycle radio-frequency (RF) pulse train with a high frequency carrier is important for ultra-wideband radars [16] and for arbitrary waveform generation [17].

To obtain short pulses from a self-sustained oscillator, several cavity modes should be locked and hence the cavity length of the oscillator should be longer than the pulse carrier wavelength. In a pioneer work, passive mode-locking of an electronic oscillator has been demonstrated [18]. The saturable absorber was implemented by using an expander based on a tube. The effect of the difference between the group and the phase velocities on short pulses has been studied. Optoelectronic oscillators offer significant advantages in compared with electronic oscillators that generate short RF pulses. The bandwidth of electro-optical systems is significantly wider in compare with that of electronic systems. Therefore, optoelectronic oscillators enable shortening the generated pulses, increasing the carrier frequency, and increasing the pulse bandwidth as required in modern ultra-wideband radars [16]. The loss of optical fibers is significantly smaller in compare with electronic transmission lines. Therefore, optoelectronic oscillators enable decreasing the repetition rate of the pulse train while maintaining low jitter as required in radar applications.

In this paper, we demonstrate experimentally the generation of low-jitter single-cycle pulse train with a carrier frequency in the RF region by using passive mode-locking of an OEO. It is the first time that single-cycle pulses are generated directly by a passive mode-locked oscillator. It is also the first time that passive mode-locking is demonstrated in an OEO. In this device pulses are amplified by an RF amplifier as in electronic oscillators. The insertion of a 200 m long fiber into the cavity enables obtaining mode-locking since it increases the cavity length without adding a significant loss. The long cavity enables the simultaneous oscillation of several modes as required in mode-locking technique. The mode-locking of the OEO enables obtaining low timing jitter — less than 5 ppm of the round-trip duration. An autonomous carrier-envelope phase locking is obtained and hence the pulse waveform is repeated each round-trip. In lasers, such locking requires adding an external feedback that controls the cavity length [19].

The oscillator described in this paper opens new opportunities to explore new physical effects and to study directly the basic limitations of single-cycle mode-locked oscillators. For example, mode-locked OEOs can be used to find the conditions for the cavity dispersion that allow the generation of single-cycle pulses and allow autonomous locking of the group and the phase velocities. In ultrashort lasers the measurement of the optical pulses gives indirect result on the electric field and it also requires many pulses. Therefore, it can not be implemented in real-time. The passively mode-locked OEO reported in this paper is based on similar effects as used to generate ultrashort optical pulses. However, the RF pulse waveform along the cavity can be measured directly. The use RF components in OEOs also enable to tailor the oscillator dispersion. We note that the generation of ultra-wideband RF pulses and single-cycle pulses has been demonstrated by using optical systems that are based on the combination of a nonlinear effect and an optical filter [20–22]; however, the noise obtained in such systems is higher than the noise obtained in passive mode-locked devices where the noise can be close to its quantum limit value [3].

2. Experimental Setup

Figure 1 describes our experimental setup. Light from a semiconductor laser with an optical power of $P_0 = 14$ dBm at a wavelength of 1550 nm is fed into an electro-optic Mach-Zehnder modulator (MZM) with a DC and AC half-voltages of $v_{\pi,DC} = 6$ V and $v_{\pi,AC} = 5.5$ V, respectively, an insertion loss of $\alpha = 6$ dB, and an extinction ratio of about $(1 + \eta)/(1 - \eta) = 20$ dB. The bias voltage was set to $v_B \approx 10$ V, such that low-voltage signals at the RF port are attenuated. The maximum attenuation was obtained for $v_B = -1$ and 11 V. The modulated light power at the output of the MZM, $P_{\text{mod}}(t)$, is related to the signal at the RF input of the MZM, $v_{\text{in}}(t)$, by [11]

$$P_{\text{mod}}(t) = (\alpha P_0/2) (1 - \eta \sin\{\pi[v_{\text{in}}(t)/v_{\pi,AC} + (v_B - v_P)/v_{\pi,DC}]\}), \quad (1)$$

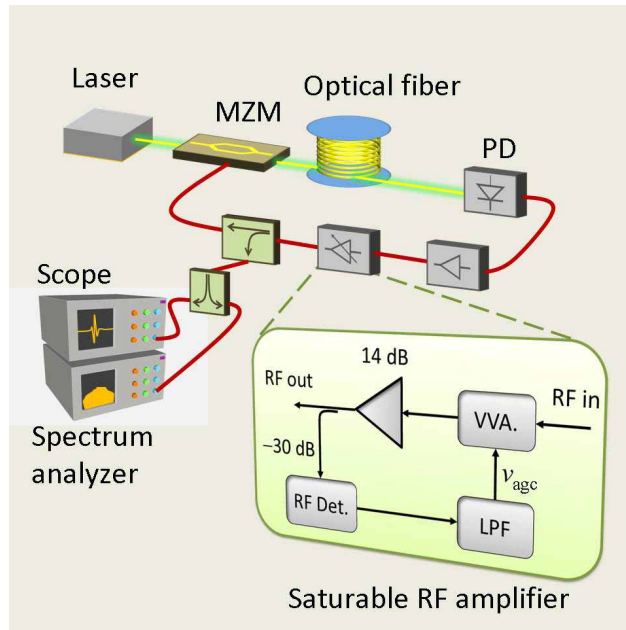


Fig. 1. Schematic description of the experimental setup. Light from a continuous wave semiconductor laser is fed into an electro-optic Mach-Zehnder modulator (MZM). The modulated light is sent through a 200 m length fiber and is then detected by using a fast photodetector (PD). The detector output is amplified by a non-saturable RF amplifier that is connected to a saturable amplifier. The amplifier output is fed back through a coupler into the RF port of the MZM to close the loop. The inset describes schematically the saturable RF amplifier: an RF signal is fed into a variable-voltage-attenuator (VVA) and is then amplified by using an RF amplifier. The RF power at the output of the amplifier is tapped out by an RF detector and is filtered by a low-pass-filter (LPF) with a cutoff frequency of 100 kHz. This signal controls the attenuation of the VVA.

where $v_P = 8$ V. The modulated light is coupled through an optical coupler to tap out 10% of the optical signal for measurements. The remind 90% of the optical signal is sent through a long fiber with a length of approximately 200 m, and is then detected by using a photo-detector with a voltage bandwidth of 15 GHz. The output electrical signal is amplified by an RF amplifier with a 19 dB gain, followed by a saturable amplifier with a maximal gain of 13.7 dB that is described in details in the next paragraph. The output of the amplifier is fed back into the RF port of the MZM through an RF coupler. The coupler was used to tap out -18.7 dB of the RF signal power to measure the signal both by a real-time scope and an RF spectrum analyzer. By using a network analyzer we measured that the coupler adds a 90° phase-shift to the tapped signal with respect to the signal that is fed to the modulator input.

The inset in Fig. 1 describes schematically the slow-saturable RF amplifier: an RF signal is fed into a variable-voltage-attenuator (VVA) and is then amplified by using an RF amplifier with 13.7 dB gain and maximal output power of 1.6 W. About 0.1% of the RF power at the output of the RF amplifier is tapped out and detected by an RF detector. The relation between the tapped power, P_t , and the voltage at the output of the RF detector is $v_{\text{out}} = aP_t(\text{dBm}) + b$, where, $a = 0.04$ V/dBm, $b = 2.5$ V, and the tapped power, P_t , is given in dBm. The rise time of the detector is about 40 ns. The output voltage is filtered by a low-pass-filter (LPF) with a cutoff frequency of 100 kHz, and is amplified by using an operational amplifier such that

$v_{\text{agc}} = c\bar{v}_{\text{out}} + d$, where \bar{v}_{out} is the voltage at the output of the LPF, $c = 4.4$, $d = 1.5$ V, and v_{agc} is the automatic gain control voltage. The voltage v_{agc} is fed back into the control port of the VVA to set its attenuation. The attenuation of the VVA (in dB) varies approximately linearly between 0 – 5 dB as a function of v_{agc} that is in the region of 0 – 2.2 V. The response time of the LPF should be longer than the round-trip time, about 1 μs , in order that the gain saturation will depend on the average RF power of the signal. Higher average RF power at the input of the saturable RF amplifier results in a higher attenuation due to the VVA, and consequently, lower the total amplification. Thus, the saturation of the RF amplifiers depends on the average signal power and it changes over a time scale that is about 10 times longer than the roundtrip duration.

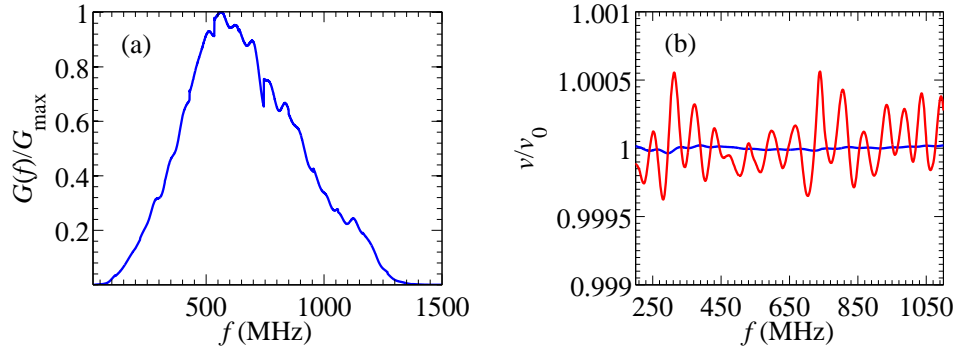


Fig. 2. (a) Gain spectrum of the saturable RF amplifier, normalized to the maximal gain $G_{\text{max}} = 13.7\text{dB}$. (b) Comparison between the phase velocity v_{phase} (blue) and the group velocity v_g (red) in one roundtrip that are normalized to $v_0 = 2.11 \cdot 10^8$ m/s. The relative difference between the phase velocity and the group velocity has an oscillatory structure in the frequency domain, with a maximal amplitude of about $\pm 0.05\%$ and a period of about 60 MHz. The high-frequency oscillation of the group velocity over a frequency octave of 440–880 MHz allows autonomous locking of the relative phase between the pulse envelope and the carrier wave as obtained in the experiments.

The bandwidth of the pulses was mainly determined by the bandwidth of the saturable RF amplifier that was about 550 MHz (full-width-at-half-maximum) around a central frequency of 600 MHz. The bandwidth of the other RF components is considerably wider (about 5 GHz). We used a network analyzer to measure the frequency response of the saturable RF amplifier. The gain spectrum, $G(f)$, normalized to the maximal gain, $G_{\text{max}} = 13.7$ dB, is shown in Fig. 2(a). The measured phase response of the saturable RF amplifier between 200 MHz and 1100 MHz equals $\varphi(f) = -2\pi f\tau_D + \psi(f)$, where $\tau_D \cong 10$ ns is an average delay that is added by the amplifier, and $|\psi(f)| \ll 2\pi$. The other components in the cavity add a delay that is approximately equal to the delay of the optical fiber, $\tau_F \cong 938$ ns. The phase and the group velocities along one roundtrip can be calculated by $v_{\text{phase}}(f) = 2\pi L/[2\pi\tau_F - \varphi(f)/f]$, and $v_g(f) = 2\pi L/[2\pi\tau_F - d\varphi(f)/df]$, respectively, where $L \approx 200$ m is the length of the optical fiber. Figure 2(b) shows a comparison between the phase velocity and the group velocity, where the two velocities are normalized by $v_0 = 2.11 \cdot 10^8$ m/s. The frequency dependence of the relative difference between the phase and the group velocities has an oscillatory behavior, with a maximal difference of about $\pm 0.05\%$ and a period of about 60 MHz. The high frequency oscillation of the group velocity over a frequency octave of 440–880 MHz allows the locking of the relative phase between the pulse envelope and the carrier phase as it is obtained in the experiments and as it is also obtained in our theoretical model that will be published elsewhere. The locking of the relative phase between the pulse envelope and the carrier phase is promoted

since it lowers the loss because a pulse with minimal loss can propagate in the cavity. As a result, the locking between the two velocities is obtained in our system autonomously.

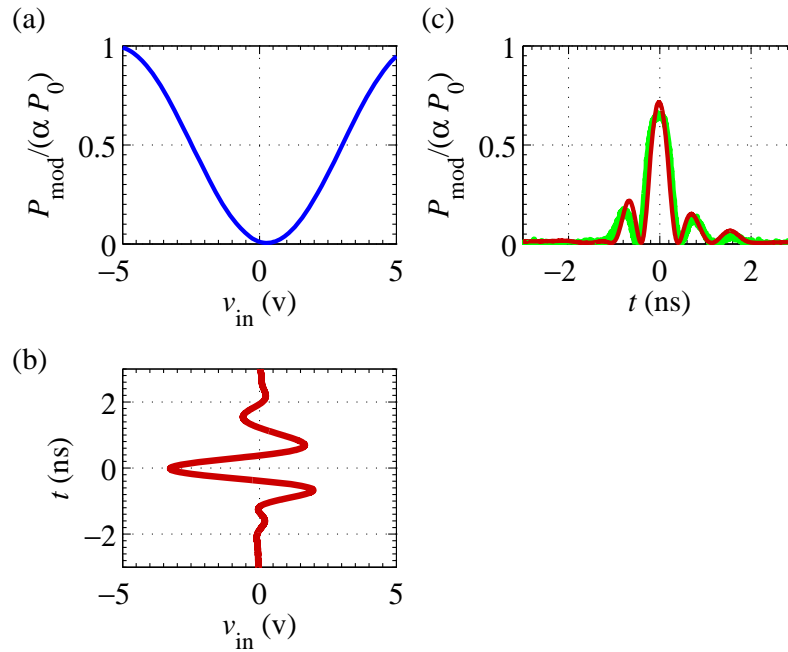


Fig. 3. (a) The transmission curve of the MZM calculated by using Eq. (1) for a bias voltage $v_B=10.7$ V. (b) Waveform at the RF port of the modulator. The waveform was obtained by measuring the pulse at the output port of the coupler by using a real-time oscilloscope, adding 18.7 dB and shifting the phase waveform by 90° . (c) Normalized optical power at the output of the MZM, $P_{\text{mod}}(t)/(\alpha P_0)$ (defined in Eq. (1)), that is measured by using a 10% optical coupler that is connected to the output port of MZM and measuring the optical signal by using a sampling oscilloscope with an average of 256 samples (green-line). The optical waveform is compared to that calculated by multiplying the waveform at the input of the MZM by its transfer curve (red-line).

The bias voltage of the modulator is set such that its transmission increases as the input voltage increases, as shown in Fig. 3(a). The figure also show that the modulator attenuates low amplitude peaks in the input waveform. Therefore, the modulator is a fast saturable absorber with a time response that is significantly shorter than the pulse duration. The gain saturation of the RF amplifiers occurs over a time scale that is about three to four orders of magnitude longer than the pulse duration. Therefore, the gain saturation of the RF amplifiers approximately depends on the average power. The combination of the modulator and the slow saturation of the RF amplifier promotes the generation of single-cycle pulses. Such short pulses are transmitted efficiently through the modulator due to their high peak voltage. At the same time, a single-cycle pulse that propagates in the cavity has a very low average power. As a result, the RF amplifier is nearly unsaturated and its amplification is almost maximal. The carrier frequency and the bandwidth of the pulses are mainly determined by the central frequency and the bandwidth of the saturable RF amplifier. The pulse must contain a carrier frequency since low-frequency components of the pulse can not propagate inside the cavity because they are blocked by the RF amplifiers (as shown in Fig. 2(a)). Therefore, the time average of the pulse field must be

equal to zero. When the gain is high enough, a bunch of pulses propagate in the cavity. By controlling the laser power and the bias voltage of the modulator we could control the loop gain and obtain a single-cycle pulse. For example, for $v_B = 10.5$ V, a bunch of about 50 single-cycle pulses were generated and the attenuation of the VVA was equal to 4 dB. When the bias voltage was gradually decreased to 10 V, a single-cycle pulse was generated. In this case, the voltage of the attenuator was equal to 1.3 V, the attenuation of the VVA was 3 dB, the gain of the saturable amplifier was 10.7 dB, and the total gain between the waveform at the input of the modulator and the waveform at the detector output was about 30 dB. The long fiber and the mode-locking of the pulses enable obtaining a very low-jitter.

3. Experimental Results

Figure 4 shows the single-cycle pulse train that was measured by a real-time oscilloscope and a spectrum analyzer. The single-cycle RF pulse has an envelope with a full-duration-at-half-maximum of 1.5 ns and a carrier wave with a period time of 1.5 ns. The carrier frequency is about 650 MHz. The measured spectrum that is described in Fig. 4(c) has a 5-dB bandwidth of 440 MHz between 440–880 MHz. Thus, the ratio between the highest and the lowest frequency of the pulse spectrum is greater than two, and the spectrum 5-dB bandwidth spans a frequency octave. We note that the voltage shown in Fig. 4 is the voltage at the output port of the RF coupler. The voltage at the modulator input, that is shown in Fig. 3(b), is about 7.2 times higher than the voltage shown in the Fig. 4 and is also 90° phase-shifted.

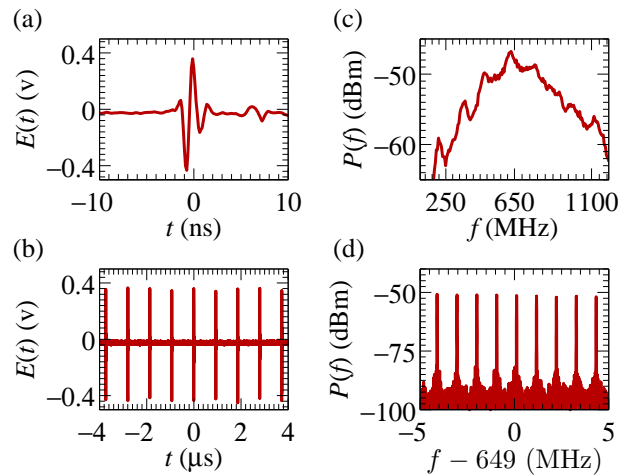


Fig. 4. Measurement of the single-cycle pulse train by using a real-time oscilloscope (a–b) and by using a spectrum analyzer (c–d). (a) single-cycle pulse waveform with a carrier period of 1.5 ns that corresponds to a carrier frequency of 650 MHz. (b) single-cycle pulse train with a period of 948.5 ns that corresponds to a repetition rate of 1.0543 MHz. (c) Envelope of the spectrum measured with a resolution bandwidth RBW = 1 MHz. (d) Oscillating modes around a frequency of 649 MHz, measured with a resolution bandwidth RBW = 10 kHz. The mode spacing of 1.0543 MHz corresponds to the time period of the pulse train. The voltage at the modulator input is 7.2 times higher than the voltage shown in the figure.

The pulse envelop propagates at the group velocity while the carrier wave propagates at the phase velocity. To obtain repetitiveness between the waveforms of adjacent ultrashort pulses there is a need to lock the relative phase between the pulse envelope and the carrier wave. In the frequency domain it means that each Fourier component is an integer multiple of the inverse of

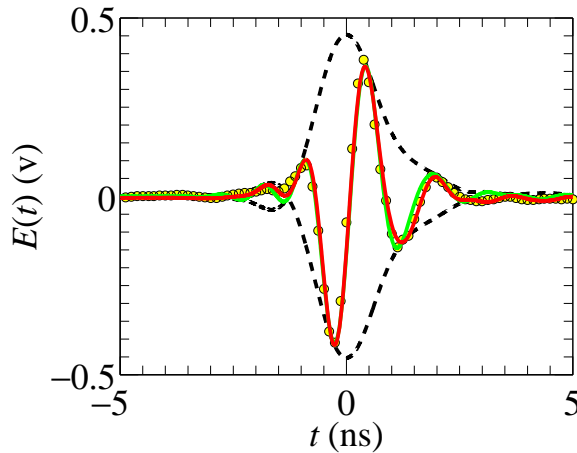


Fig. 5. Single-cycle pulse waveform as it was measured by a real-time oscilloscope (yellow circles) and by a sampling oscilloscope with an averaging of 256 samples (red solid-line). The waveform has a carrier period of 1.5 ns and its extracted envelope norm, $\pm|a(t)|$ (black dashed-line), has a full-duration-at-half-maximum of 1.5 ns. The signal that is calculated from the envelope is shown for comparison (green solid-line).

the time between adjacent pulses [19]. In case that the group and the phase velocities are not the same, the pulse shape changes from one round-trip to another [18]. By using a real-time and sampling oscilloscopes we verified that the shape of the electrical pulse in the mode-locked OEO is repeated every round-trip without a need to control the cavity length. Hence, the carrier phase and the envelope phase are locked autonomously. Locking of the carrier and the envelope phases in lasers requires adding an external feedback that controls the cavity length [19]. In the passively mode-locked OEO the locking is obtained without controlling the cavity length since the response time of the modulator is an order of magnitude shorter than the carrier period and hence a change in the pulse waveform from one round-trip to the following results in a significant increase in the loss. Furthermore, the relative difference between the measured phase and group velocities varies with a high frequency period over the entire bandwidth and with an amplitude less than 0.05%, as shown in Fig. 2(b). The rapid change of the group velocity over the pulse bandwidth, and the relatively small difference between the phase and the group velocities, allow the locking of the velocities as it is obtained in the experiments.

The width of the pulse envelope, $a(t)$, can be approximately extracted from the measured waveform $v(t) = a(t) \exp(2\pi i f_0 t)/2 + c.c.$, where f_0 is the carrier frequency. The Fourier transform of the wave equals $V(f) = [A(f - f_0) + A^*(-f_0 - f)]/2$, where $A(f)$ is the Fourier transform of $a(t)$. One part of the spectrum is located in the positive frequency region, $V_p(f)$, and the other part is located in the negative frequency region, $V_n(f)$. In a single-cycle pulse the spectrum in the positive frequency region $V_p(f)$ contains not only components of $A(f - f_0)/2$, but also components from $A^*(-f_0 - f)/2$. However, if the overlap between the negative and positive frequency components is small, we can assume that $V_p(f) \approx A(f - f_0)/2$ and $V_n(f) \approx A^*(f_0 - f)/2$. Then, the spectrum of the envelope can be obtained by $A(f) = V_p(f + f_0) + V_n^*(-f + f_0)$. By applying an inverse-Fourier-transform to $A(f)$ the envelope $a(t)$ is obtained. Figure 5 shows the extracted envelope $\pm|a(t)|$. The figure shows that the measured signal and the signal that is calculated from the envelope are similar but not identical, as it expected when the bandwidth of the signal envelope is comparable with the carrier frequency. The full-duration-at-half-maximum of the envelope equals 1.5 ns compared to 1.5 ns period of

the carrier. The time derivative of the envelope argument varies by less than 50 MHz along the time duration when $|a(t)|^2/\max(|a(t)|^2) > 0.1$.

4. Pulse to Pulse Jitter

The jitter and the stability of the pulse repetition rate of the device are determined by the noise that is added in each round-trip. By using a sampling oscilloscope, the measured pulse to pulse jitter of the pulse train was less than 5 ps which is approximately 5 ppm of the pulse repetition period of 948.5 ns. The jitter measurement was limited by the oscilloscope accuracy.

Since we do not stabilize the system, the long term stability is mainly determined by environmental changes in the fiber. The stability of the pulse repetition rate over a long time was measured by using a counter. The gate time of the counter, which determines the duration of each frequency measurement, was set to 4 seconds. The measurements were collected over a time period of about 3/4 hour. The average pulse repetition rate was equal to 1,054,301 Hz and the rate change was less than 1.5 Hz. The frequency deviations from one measurement to the following had a normal distribution with a standard deviation of $\sigma_f = 0.13$ Hz. The repetition rate deviations from one measurement to the following had a cross correlation values that were less than 0.1, which implies that different measurements were not correlated.

We calculated the pulse to pulse jitter in our system due to additive white Gaussian noise. We describe the waveform of one of the pulses in the presence of noise by $v(t) = f(t) + n(t)$, where $v(t)$ is the voltage of the waveform at the output of the amplifier, $f(t)$ is the corresponding unperturbed waveform in the absence of noise, and $n(t)$ is a real noise that is added to the pulse waveform in each round-trip. We assume that the added noise is a real Gaussian noise with a time average $\langle n(t) \rangle = 0$, and a correlation at the output of the RF amplifiers $\langle n(t)n(t') \rangle = \delta(t-t')\sigma_n^2 = \delta(t-t')G\rho_N R/2$, where G is the amplification, ρ_N is the effective power spectral density of the noise (one-sided) at the input of the amplifier, R is the load impedance, and $\delta(t)$ is the Dirac delta function. The jitter due to the noise can be calculated as performed in lasers [23, 24] or in optical communication systems [25]. Due to the small effect of dispersion on the RF pulses the main source of the jitter in the mode-locked OEO is the direct contribution of the noise to the change in the central pulse time. We define the central pulse time of one of the unperturbed pulses as

$$T_p = \int_{-\infty}^{\infty} t' f^2(t') dt' / E_0, \quad (2)$$

where E_0 is the energy of the pulse waveform

$$E_0 = \int_{-\infty}^{\infty} f^2(t') dt'. \quad (3)$$

We define a time coordinate $t = t' - T_p$ with respect to the central time of the unperturbed pulse T_p . In the presence of noise, the central pulse time becomes:

$$T = \int_{-\tau/2}^{\tau/2} t [f(t) + n(t)]^2 dt / E_0, \quad (4)$$

where τ is the round-trip time, $t \in [-\tau/2, \tau/2)$. In deriving Eq. (4) we neglect the effect of the pulse energy change due to the noise on the jitter. Keeping terms up to the first order in $n(t)$, the deviation in the central pulse time in presence of noise, equals:

$$\delta T \cong \frac{2}{E_0} \int_{-\tau/2}^{\tau/2} t f(t) n(t) dt, \quad (5)$$

The random variable δT changes from one round-trip to the other. The standard deviation of δT is defined as the jitter. Since the added noise is a white Gaussian noise that is delta-correlated

in time, the deviation of the central pulse time, δT , is normally distributed with a standard deviation of

$$\sigma_{\tau} = \frac{2}{E_0} \sqrt{(G\rho_N R/2) \int_{-\tau/2}^{\tau/2} t^2 f^2(t) dt}. \quad (6)$$

We estimated the minimal theoretical pulse to pulse jitter in our system. We assume that the power spectral density of the noise, ρ_N , is dominated by two unavoidable noise sources: thermal noise of the RF amplifiers, $\rho_{th} = NF \cdot k_B T_{amb}$, and shot noise, $\rho_{SN} = 2q_e I_{PD} R$, such that $\rho_N = \rho_{th} + \rho_{SN}$, where k_B is the Boltzmann constant, T_{amb} is the ambient temperature, NF is the noise factor of the RF amplifiers, q_e is the electron charge, and I_{PD} is the photocurrent. In our system $R = 50 \Omega$, $I_{PD} = 4 \text{ mA}$, and $G = 32 \text{ dB}$. In the case of an ideal RF amplifier $NF = 1$, and for $T_{amb} = 300 \text{ }^\circ\text{K}$, the spectral noise density equals to $\rho_N = 7 \cdot 10^{-20} \text{ W/Hz}$. Therefore, the resulting timing jitter calculated by using Eq. (6) equals $\sigma_{\tau} = 0.6 \text{ ps}$.

5. Conclusions

Single-cycle pulses are the shortest pulses that can be obtained for a given carrier frequency. We have demonstrated the generation of single-cycle RF pulses by passive mode-locking of an OEO. Our measurements indicate that an autonomous locking of the carrier phase with respect to the envelope phase is achieved, so that the pulse waveform is preserved in each round-trip. The measured pulse train has a low pulse to pulse jitter, less than 5 ppm of the round-trip duration. The method described here enables generating single-cycle RF pulse train with a low repetition rate and a low jitter which could not be generated till now by electronic systems. The carrier frequency of the OEO reported in this paper is 650 MHz. However, the method is directly scalable to higher frequencies, and it is limited today only by the maximum frequency of optoelectronic components, which is of the order of tens of GHz.

The low-jitter pulses that are generated by the mode-locked OEO are important for many radar applications, such as in ultra-wideband radars [16], and in bistatic or multistatic radars, in which the transmitting and the receiving antennas are separated [26]. In such radars the synchronization between the transmitting and receiving antenna can be dramatically improved by using a low jitter pulse source. Ultra-low-jitter short pulses can also enable the development of novel radars. Ultra-wideband pulses are required to improve the spatial resolution of radars, and single-cycle pulses are the shortest pulses that can be obtained for a given carrier frequency. Doppler radars transmit signals with a long duration and a low phase noise to accurately measure the velocity of moving objects. Very short pulses with a low jitter, as generated by the system described in this paper, can be used to develop novel radars that will be able to accurately measure both range and velocity. Low-jitter single-cycle pulses are also important for generating RF pulses with an arbitrary waveform due to their ultra-wide bandwidth.

Acknowledgments

This work was supported by the Israel Science Foundation (ISF) of the Israeli Academy of Sciences. The authors are highly grateful to C. R. Menyuk for fruitful discussions and useful remarks.